



## **Effect of Spinning Rate on Structure and Morphology of ZnO:Cu Thin Films Prepared using a Sol-gel Spin Coating Method**

**Nur Hamid, Budi Astuti\*, Ngurah Made Dharma Putra, Putut Marwoto, Sugianto, Rodhotul Muttaqin, Natalia Erna Setyaningsih**

Department of Physics, Faculty of Mathematics and Sciences, Universitas Negeri Semarang  
Bld. D7, Sekaran Campus, Gunungpati, Semarang, Central Java, Indonesia, 50229

\*Corresponding author e-mail: [b\\_astuti79@mail.unnes.ac.id](mailto:b_astuti79@mail.unnes.ac.id)

DOI: <https://doi.org/10.15294/ijrie.v1i1>

Accepted: March 12, 2020. Approved: June 15, 2020. Published: July 30, 2020

### **ABSTRACT**

Cu-doped ZnO (ZnO:Cu) thin film was deposited on glass substrate using a sol-gel spin coating method. The film was prepared at various spinning rate followed by sintering at 250 °C for 10 min and annealing at 350 °C for 2 hours. The effect of spinning rate on structural properties was investigated by means of X-ray diffractometer (XRD), scanning electron microscope (SEM) equipped with energy dispersive X-ray (EDX). The diffraction pattern indicated that Cu-ZnO thin films showed a strong c-axis orientation, i.e. the peak attributed to (002) plane at a  $2\theta$  of  $34.42^\circ$  corresponding to hexagonal wurtzite crystals. An increase in the spinning rate resulted in ZnO:Cu thin films with high homogeneity. It was further proved by SEM and EDX results.

**Keywords:** ZnO:Cu; thin film; spinning rate; sol-gel spin coating.

© 2020 Innovation Center LPPM UNNES Semarang

### **1. INTRODUCTION**

Thin film technology continues to develop towards cheap and environmentally friendly materials that are easy in large-scale production (Harish et al., 2019). In addition, a good structure with optical, electrical and magnetism properties is required for good thin films (Ammaih et al., 2014). The development of thin film technology has been applied to solar cells (Tumbul et al., 2019), transparent conductive oxide (TCO)

(Mughal et al., 2017), photocatalysts (Kaviyarasu et al., 2017), transistors (Ruzgar & Caglar, 2019), super capacitors (Hassan et al., 2019) and others. Recently, researchers have paid more attention zinc oxide (ZnO); a II-VI inorganic semiconductor. Wurtzite structure of ZnO with a lattice spacing  $a$  of 3.25 Å and  $c$  of 5.21 Å has a bandgap width of 3.4 eV and melting point of 2,248 K (Arif et al., 2018). However, ZnO shows weaknesses in their electrical properties. In order to overcome this issue, the addition of doping from transition

metals such as copper (Cu) is an effective method (El-Hilo et al., 2009; Marwoto et al., 2012).

Several methods of growing thin films have been developed such as RF magnetron sputtering (Samavati et al., 2016), DC magnetron sputtering (Zhu et al., 2015), spray pyrolysis (Mimouni et al., 2015), metalorganic chemical vapor deposition (MOVCD) ( Li et al., 2019), molecular beam epitaxy (MBE) (Darma et al., 2019), pulsed laser deposition (PLD) (Zawadzka et al., 2016) and sol-gel spin coating (Leelaruedee et al., 2019). Sol-gel spin coating is very promising method in the thin film preparation due to its easy and inexpensive process, as well as feasible to large scale production (Arif et al., 2018; Nimbalkar & Patil, 2017). The effectiveness of this method is significantly influenced by several factors such as rotation speed and time. This rotational speed per minute was reported to affect the surface morphology, subsurface defects and impurity content of the thin films (Ilican et al., 2008).

This paper discussed about the effect of spinning rate on the structure and morphology of the prepared ZnO:Cu thin films. The thin films were grown on glass substrates and sintered to form new compounds and crystal structures. The surface structure and morphology of the thin films were investigated by using X-ray diffraction (XRD) and scanning electron microscope (SEM) equipped with energy dispersive X-ray (EDX), respectively.

## 2. METHODS

Zinc acetate dihydrate  $Zn(CH_3COO)_2 \cdot 2H_2O$ , AZD and copper(II) acetate monohydrate  $Cu(CH_3COO)_2 \cdot H_2O$ , CAM were of analytic grade with a purity around 99.99% and utilized as the precursor. 2-Propanol  $CH_3CH(OH)CH_3$  and monoethanolamine  $NH_2CH_2CH_2OH$ , MEA were used as solvent and stabilizer, respectively. All the chemicals were obtained from Merck KGaA, 64271 Darmstadt (Germany). The precursor solutions were prepared at 0.5 M by mixing 2.17 g of  $Zn(OAc)_2$  and 0.02 g  $(Cu(OAc)_2)$  in 20 mL of 2-propanol and stirred using a magnetic stirrer. After stirring for 15 minutes at 60 °C, 0.62 mL of MEA was added to the solution under stirring at a constant rate. The final solution was stirred at the same temperature (60 °C) for another 60 minutes.

The final solution was a highly homogeneous and transparent blue color solution. The solution was then left for 24 hours at room temperature to ensure there was no any precipitate in the solution. At the same time, a cleaning process of the glass substrate was done using acetone for 15 minutes and methanol for 5 minutes in an ultrasonic bath. The glass substrate was dried by flowing nitrogen gas. Afterward, the solution was dropped on the glass substrate and spined at various spinning rate i.e. 2600, 2800, 3000, 3200, and 3400 rpm for 15 seconds. The resulted ZnO:Cu thin films were thermally sintered at 250 °C for 15 minutes and annealed at 350 °C for 2 hours. The structural properties and orientation of the ZnO:Cu thin films were investigated by means of x-ray diffractometer (XRD) using a  $Cu K_\alpha$  radiation ( $\lambda = 1.542 \text{ \AA}$ ). The lattice constants  $a$  and  $c$  of the hexagonal wurtzite structure of ZnO film with (002) orientation were calculated using equations (1) and (2) (Kahouli et al., 2015; Poongodi et al., 2015).

$$a = \frac{\lambda}{\sqrt{3} \sin \theta} \quad (1)$$

$$c = \frac{\lambda}{\cos \theta} \quad (2)$$

The results of the lattice constant  $a$  and  $c$  based on calculation are similar to JCPDS reference number. The crystallite size,  $D$  was calculated by the Debye-Scherrer's equation (Equation (3)).

$$D = \frac{K\lambda}{\beta \cos \theta} \quad (3)$$

where  $K$  is the Scherrer constant (0.89),  $\lambda$  (1.542 Å) is the wavelength of radiation,  $\beta$  is FWHM and  $\theta$  is the peak position of XRD. Then, the dislocation density,  $\delta$  was obtained using equation (4).

$$\delta = \frac{1}{D^2} \quad (4)$$

The surface morphology of the prepared thin films was investigated using a scanning electron microscope (SEM) equipped with an energy dispersive X-ray (EDX) to determine the elemental composition of the obtained ZnO:Cu thin films.

**3. RESULTS AND DISCUSSION**

**3.1. Structural Study**

The direction of crystal orientation and the structure of the ZnO:Cu thin film crystals were examined using XRD. The XRD patterns of the ZnO:Cu thin films made prepared by the sol-gel spin coating method with different spinning rate i.e. 2400, 2600, 3000, 3200 and 3400 rpm are shown in **Figure 1**. Three dominant peaks that corresponded to plane (100), (002), and (101) were observed in the XRD patterns. Those closely matched with the JCPDS data i.e. 01-078-3315 and 76-0704 indicating that the prepared ZnO:Cu thin films showed a polycrystalline structure. The data also indicated that the prepared ZnO:Cu thin films had a hexagonal wurtzite structure (Astuti, et al., 2019; Khosravi, et al., 2019). The XRD patterns in

**Figure 1** also indicated that all of the prepared thin films had no preferred orientation. This might be due to the preferred orientation was weakened and the rotation speed on the spinning process might have no effect on the crystal orientation.

This study would like to focus on (002) peak because the crystal with (002) orientation plane could be applied as a window layer on the solar cell technology. A window layer material should have a high transmittance and a wide band gap energy. Previous study reported that (002) ZnO thin films showed a high transferability of 80-90% (Bedia et al., 2015; Rahmane et al., 2015), while the optical properties of the prepared ZnO:Cu thin films would be discussed later in the next study. The lattice constants and crystallite size of the ZnO:Cu thin films are presented in **Table 1**.

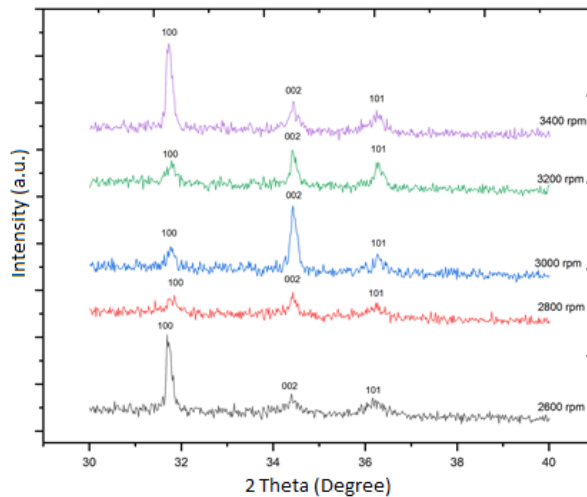


**Figure 1.** XRD patterns for ZnO:Cu thin films prepared using a sol-gel spin coating method with various spinning rates (2400-3400 rpm).

**Table 1.** Structural and lattice parameters of the ZnO:Cu thin films prepared using sol-gel spin coating method with various spinning rates of 2400-3400 rpm.

Spinning rate (rpm)	2θ (°)		FWHM (°)		Lattice constants (Å)		d (nm)	D (nm)	σ (nm <sup>2</sup> )	Lattice constants from JCPDS (Å)	
	100	002	100	002	a (100)	c (002)				a (100)	c (002)
2600	31.70	34.42	0.16	0.20	3.26	5.21	2.61	42.30	0.00056	3.25	5.21
2800	31.76	34.46	0.20	0.16	3.26	5.21	2.60	52.89	0.00036	3.25	5.21
3000	31.80	34.43	0.12	0.12	3.25	5.21	2.60	70.49	0.00020	3.25	5.21
3200	31.8	34.44	0.16	0.16	3.25	5.21	2.60	52.89	0.00036	3.25	5.21

**3.2. Surface Morphology**

The surface morphology of the ZnO:Cu thin films prepared using a sol-gel spin coating method with different spinning rate (2600, 2800, 3000, 3200, and 3400 rpm) was analyzed by using scanning electron microscope (SEM) equipped with an EDX to reveal the elemental composition. **Figures 2** shows the change in the surface morphology of the ZnO:Cu by increasing the spinning rate. The SEM micrographs in **Figure 2** indicated that an inhomogeneous and dense structure (Arif et al., 2018). The agglomeration of particles was observed in all micrographs (see Figure 2). It was clearly shown in **Figure 2** that the ZnO:Cu thin film with a spinning rate of 3000 rpm showed a higher uniformity compared to the other thin films prepared in this study. This was well-confirmed by the XRD patterns presented earlier in **Figure 1**.

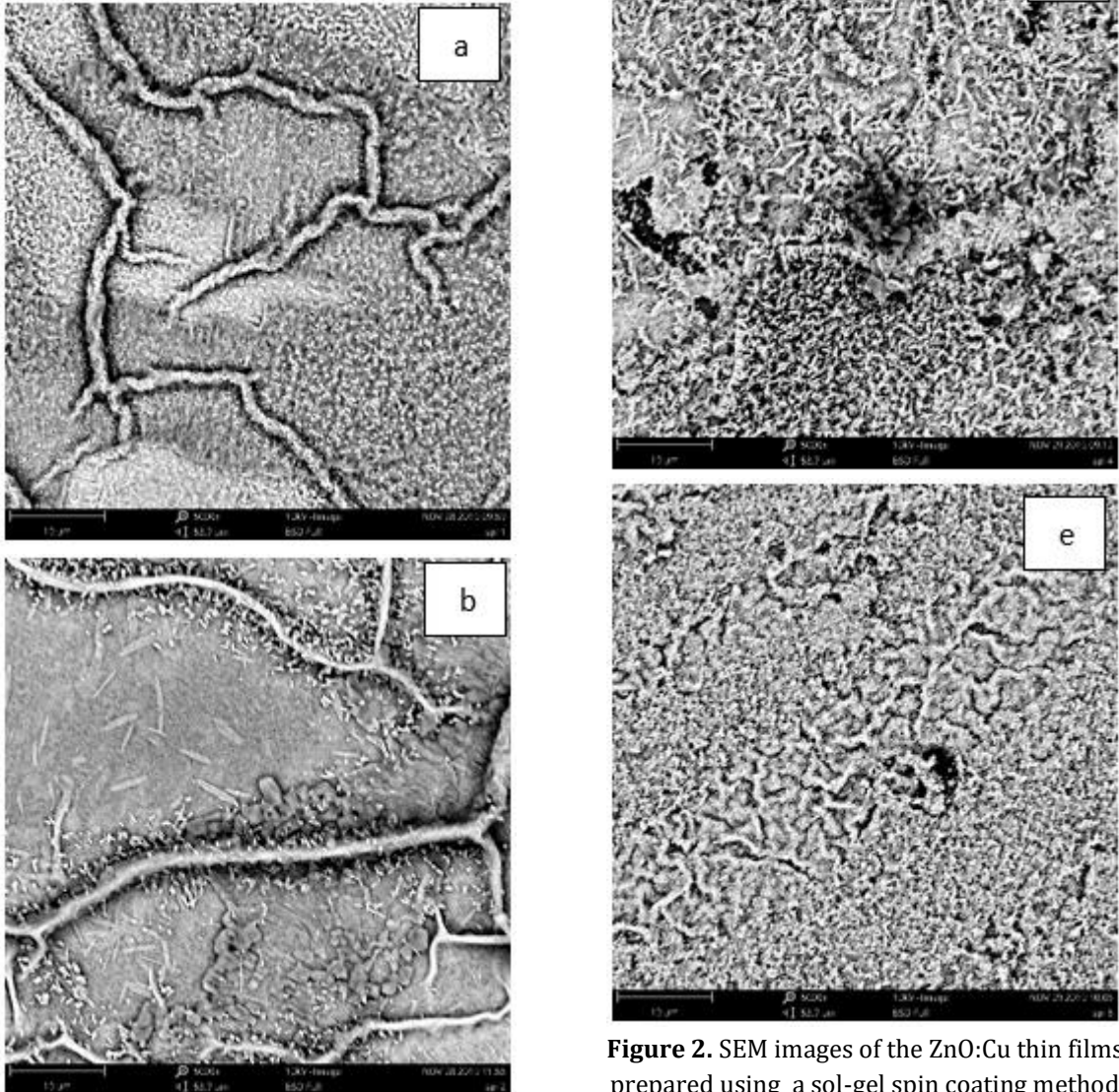


**Figure 2.** SEM images of the ZnO:Cu thin films prepared using a sol-gel spin coating method with a spinning rate of (a) 2400 (b) 2600 (c) 3000 (d) 3200 and (e) 3400 rpm.

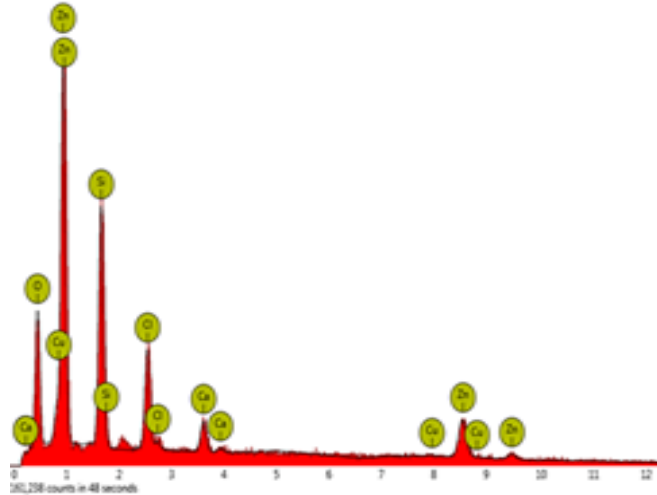


**Figure 3.** EDX result of the ZnO:Cu thin films prepared using a sol-gel spin coating method with various spinning rate (2400-3400 rpm).

**Table 2.** Elemental composition of the ZnO:Cu thin films prepared using a sol-gel spin coating method with various spinning rate (2400-3400 rpm).

Spinning rate (rpm)	Elemental Concentration (%)					
	O	Zn	Si	Cl	Ca	Cu
2600	39.52	32.56	12.99	12.8	1.6	0.52
2800	50.98	20.23	19.06	7.03	2.36	0.34
3000	50.84	30.26	14.48	2.07	1.78	0.57
3200	53.06	29.71	7.98	7.53	1.30	0.42
3400	47.91	38.07	10.31	1.95	1.41	0.35

Stoichiometry and elemental composition of the ZnO:Cu thin films were carried out using an energy dispersive X-ray (EDX) spectrometer. The results are shown in **Figure 3** and **Table 2**. The EDX result in **Figure 3** confirmed the presence of Zn, O and Cu elements in the ZnO:Cu thin film prepared in this study. In addition, the contaminants such as Si, Cl and Ca elements were also observed in the EDX result. The observed Si element was expected come from the substrate due to the thin samples during analysis. Furthermore, the observed Cl and Ca elements were likely coming from the raw material used during the synthesis of the thin films. **Figure 3** also shows that Cu element showed a high peak intensity at the same point as Zn did. It might indicate that Cu atoms substituted several Zn atoms in the ZnO matrix (Hanh et al., 2019). All samples appeared to contain Cu elements indicating that Cu dopant has entered the ZnO bond. Finally, it also indicated that the spinning rate in the sol-gel spin coating method might only affect the

structure properties such as uniformity, FWHM, crystallite size, that would further affect the film quality.

#### 4. CONCLUSIONS

The ZnO:Cu thin films grown using a sol-gel spin coating method has been carried out with different spinning rates (2400-3400 rpm). The XRD patterns indicated that the resulted ZnO:Cu thin films had a hexagonal wurtzite structure with a dominant orientation of (002) plane. The morphology of the film prepared with the spinning rate of 3000 rpm showed a higher uniformity compared to those with other spinning rates. The presence of Cu, Zn and O elements along with the concentration of each element in the prepared ZnO:Cu thin films was observed based on the EDX results. The Cu atoms likely substituted several Zn atoms in the ZnO matrix. Cu atoms were observed in all ZnO:Cu thin films. The highest concentration Cu atoms with was

observed in the ZnO:Cu thin films prepared with a spinning rate of 3000 rpm.

## 5. REFERENCES

- Amakali, T., Daniel, L.S., Uahengo, V., Dzade, N.Y. & de Leeuw N.H. 2020. Structural and optical properties of ZnO thin film prepared by molecular precursor and sol-gel method. *Crystal*, 10(2):132. <https://doi.org/10.3390/cryst10020132>.
- Ammaih, Y., Lfakir, A., Hartiti, B., Ridah, A., Thevenin, P. & Siadat, M. 2014. Structural, optical and electrical properties of ZnO:Al thin films for optoelectronic applications. *Optical and Quantum Electronics volume, 46*: 229–234. <https://doi.org/10.1007/s11082-013-9757-2>.
- Arif, M., Sanger, A., Vilarinho, P. M. & Singh, A. 2018. Effect of annealing temperature on structural and optical properties of sol-gel-derived ZnO thin films. *Journal of Electronic Materials*, 47(7): 3678–3684. <https://doi.org/10.1007/s11664-018-6217-6>
- Astuti, B., Sugianto, Maftuchah, I., Firmahaya, N.A., Marwoto, P., Ratnasari, F.D., Muttaqin, R. Setyaningsih, N.E., Aryanto, D. & Isnaeni. 2019. Photoluminescence study of ZnO:Al thin film with different power plasma. *Journal of Physics Conference Series*, 1321(2): 1-6. <https://iopscience.iop.org/article/10.1088/1742-6596/1321/2/022009>.
- Bedia, A., Bedia, F.Z., Aillerie, M., Maloufi, N. & Benyoucef, B. 2015. Morphological and optical properties of ZnO thin films prepared by spray pyrolysis on glass substrates at various temperatures for integration in solar cell. *Energy Procedia*, 74: 529–538. <https://doi.org/10.1007/s10854-017-7562-6>.
- Darma, Y., Muhammady, S., Hendri, Y.N., Sustini, E., Widita, R. & Takase, K. 2019. Tuning the point-defect evolution, optical transitions, and absorption edge of zinc oxide film by thermal exposure during molecular beam epitaxy growth. *Materials Science in Semiconductor Processing*, 93: 50-58. <https://doi.org/10.1016/j.mssp.2018.12.030>.
- El-Hilo, M., Dakhel, A.A. & Ali-Mohamed, A.Y. 2009. Room temperature ferromagnetism in nanocrystalline Ni-doped ZnO synthesized by co-precipitation. *Journal of Magnetism and Magnetic Materials*, 321(14): 2279–2283. <https://doi.org/10.1016/j.jmmm.2009.01.040>.
- Hanh, N.T., Tri, N.L.M., Thuan, D.V., Tung, M.H.T., Pham, T.D. Minh, T.D. Trang, H.T., Binh M.T. & Nguyen, M.V. 2019. Monocrotophos pesticide effectively removed by novel visible light driven Cu doped ZnO photocatalyst. *Journal of Photochemistry & Photobiology, A: Chemistry*, 382: 111923. <https://doi.org/10.1016/j.jphotochem.2019.111923>.
- Harish, S.V., Suhas, S.A., Harish, S. & Vinayaka, R. 2019. Solar panel maintenance system. *International Journal of Industrial and Systems Engineering*, 1(2): 88–92. Retrieved from [www.sikhiva.org](http://www.sikhiva.org)~88~
- Hassan, K., Farzana, R. & Sahajwalla, V. 2019. In-situ fabrication of ZnO thin film electrode using spent Zn-C battery and its electrochemical performance for supercapacitance. *SN Applied Sciences*, 1(4): 302-314. <https://doi.org/10.1007/s42452-019-0302-1>.
- Ilican, S., Caglar, Y., Caglar, M. & Yakuphanoglu, F. 2008. Structural, optical and electrical properties of F-doped ZnO nanorod semiconductor thin films deposited by sol-gel process. *Applied Surface Science*, 255(5): 2353-2359. <https://doi.org/10.1016/j.apsusc.2008.07.111>.
- Kahouli, M., Barhoumi, A., Bouzid, A., Al-Hajry, A. & Guermazi, S. 2015. Structural and optical properties of ZnO nanoparticles prepared by direct precipitation method. *Superlattices and Microstructures*, 85: 7–23. <https://doi.org/10.1016/j.spmi.2015.05.007>.
- Kaviyarasu, K. Magdalane, C.M., Kanimozhi, K,

- Kennedy, J., Siddhardha, B., Reddy, E., Rotte, N.K., Sharma, C.S. Thema, F.T., Letsholathebe, D., Mola, G.T. & Maaza, M. 2017. Elucidation of photocatalysis, photoluminescence and antibacterial studies of ZnO thin films by spin coating method. *Journal of Photochemistry & Photobiology, B: Biology*, 173: 466-475. <https://doi.org/10.1016/j.jphotobiol.2017.06.026>.
- Khosravi, P., Karimzadeh, I. & Salimijati, H.R. 2019. Investigation of structural and optical properties of ZnO:Cu co-sputtered thin film. *Material Research Express*, 6(11):116420. <https://iopscience.iop.org/article/10.1088/2053-1591/ab4493/meta>.
- Leelaruedee, K., Visuttipitukul, P. & Yongvanich, N. 2015. Effect of heating rate on morphology of anti-reflective tio2 film coated by sol-gel with poly(ethylene glycol). *Journal of Metals, Materials and Minerals*, 25(1): 51-60.
- Li, J., Wu, Z., Xu, Y., Pei, Y. & Wang, G. 2019. Stability analysis of multi process parameters for metal-organic chemical vapor deposition reaction cavity. *Molecules*, 24(5): 876-886. <https://doi.org/10.3390/molecules24050876>.
- Marwoto, P., Darmaputra, N.M., Sugianto, Othaman, Z., Wibowo, E. & Astuti, S.Y. 2012. Peningkatan kualitas film tipis CdTe sebagai absorber sel surya dengan menggunakan doping tembaga (Cu). *Jurnal Pendidikan Fisika Indonesia*, 8(2): 1-7.
- Mimouni, R., Kamoun, O., Yumak, A., Mhamdi, A., Boubaker, K., Petkova, P. & Amlouk, M. 2015. Effect of Mn content on structural, optical, opto-thermal and electrical properties of ZnO:Mn sprayed thin films compounds. *Journal of Alloys and Compounds*, 645: 100-111. <https://doi.org/10.1016/j.jallcom.2015.05.012>.
- Mughal, A.J., Carberry, B., Speck, J.S. Nakamura, S. & Denbaars, S.P. 2017. Structural and optical properties of group III doped hydrothermal ZnO Thin Films. *Journal of Electronic Materials*, 46: 1821-1825. <https://doi.org/10.1007/s11664-016-5235-5>.
- Nimbalkar, A.R. & Patil, M.G. 2017. Synthesis of highly selective and sensitive Cu-doped ZnO thin film sensor for detection of H2S gas. *Materials Science in Semiconductor Processing*, 71: 332-341. <https://doi.org/10.1016/j.mssp.2017.08.022>.
- Poongodi, G., Kumar, R. M. & Jayavel, R. 2015. Structural, optical and visible light photocatalytic properties of nanocrystalline Nd doped ZnO thin films prepared by spin coating method. *Ceramics International*, 41(3): 4169-4175. <https://doi.org/10.1016/j.ceramint.2014.12.098>.
- Rahmane, S., Aida, M.S., Djouadi, M.A. & Barreau, N. 2015. Effects of thickness variation on properties of ZnO:Al thin films grown by RF magnetron sputtering deposition. *Superlattices and Microstructures*, 79: 148-155. <https://doi.org/10.1016/j.spmi.2014.12.001>.
- Ruzgar, S. & Caglar, M. (2019). The effect of Sn on electrical performance of zinc oxide based thin film transistor. *Journal of Materials Science: Materials in Electronics*, 30(1): 485-490. <https://doi.org/10.1007/s10854-018-0313-5>.
- Samavati, A., Nur, H., Ismail, A.F. & Othaman, Z. 2016. Radio frequency magnetron sputtered ZnO/SiO2/glass thin film: Role of ZnO thickness on structural and optical properties. *Journal of Alloys and Compounds*, 671: 170-176. <https://doi.org/10.1016/j.jallcom.2016.02.099>.
- Tumbul, A., Aslan, F., Göktaş, A., & Mutlu, I.H. 2019. All solution processed superstrate type Cu<sub>2</sub>ZnSnS<sub>4</sub> (CZTS) thin film solar cell: effect of absorber layer thickness. *Journal of Alloys and Compounds*, 781: 280-288. <https://doi.org/10.1016/j.jallcom.2018.12.012>.
- Zawadzka, A. Płóciennik, P. El Kouari, Y. Bougharraf, H. & Sahraoui, B. 2016. Linear and nonlinear optical properties of ZnO thin

films deposited by pulsed laser deposition.  
*Journal of Luminescence*, 169(B): 483-491.  
<https://doi.org/10.1016/j.jlumin.2015.04.020>.

Zhu,K, Yang, Y. & Song, W. 2015. Effects of substrate temperature on the structural, morphological, electrical and optical properties of Al and Ga co-doped ZnO thin films grown by DC magnetron sputtering. *Materials Letters*, 145: 279-282.  
<https://doi.org/10.1016/j.matlet.2015.01.130>.